EMG-Based Neural Network Control of an Upper-Limb Power-Assist Exoskeleton Robot*

Hang Su[1], Zhijun Li[1,**], Guanglin Li[2], and Chenguang Yang[3]

[1] Key Lab of Autonomous System and Network Control
College of Automation Science and Engineering
South China University of Technology, Guangzhou, China
zjli@ieee.org
[2] Shenzhen Institutes of Advanced Technology
Chinese Academy of Sciences Shenzhen, Guangdong, China
gl.li@siat.ac.cn
[3] School of Computing and Mathematics
Plymouth University, U.K., PL4 8AA
chenguang.yang@plymouth.ac.uk

Abstract. The paper presents the electromyogram (EMG)-based neural network control of an upper-limb power-assist exoskeleton robot, which is proposed to control the robot in accordance with the user's motion intention. The upper limb rehabilitation exoskeleton is with high precision for co-manipulation tasks of human and robot because of its backdrivability, precise positioning capabilities, and zero backlash due to its harmonic drive transmission (HDT). The novelty of this work is the development of an adaptive neural network modeling and control approach to handle the unknown parameters of the harmonic drive transmission in the robot to facilitate motion control. We have conducted the experiments on human subject to identify the various parameters of the harmonic drive system combining sEMG information signals.

Keywords: Neural network control, sEMG, Harmonic Drive Transmission.

1 Introduction

In several countries, the increasing aging population and the decreasing working proportion has attracted much attention. In order to solve the problems associated with elders, disabled and weak people, many kinds of robot-assisted exoskeleton have been developed [1], [2]. The upper-limb robot-assisted exoskeleton

* This work is supported in part by the Natural Science Foundation of China under Grants 61174045 and 61111130208, the International Science and Technology Cooperation Program of China under Grant 2011DFA10950, and the Fundamental Research Funds for the Central Universities under Grant 2011ZZ0104, and the Program for New Century Excellent Talents in University No. NCET-12-0195.
** Corresponding author.

C. Guo, Z.-G. Hou, and Z. Zeng (Eds.): ISNN 2013, Part II, LNCS 7952, pp. 204–211, 2013.

has mainly focused on restoring arm functions to achieve many activities of daily living (ADL) such as writing/typing, personal hygiene, with the use of devices such as the MIT-MANUS [5], [3], the ARMguide [4], NeReBot[7] or the MIME [6]. Numerous promising results has been yielded that illustrate the potential of robots to complement traditional assist in physical rehabilitation. Moreover, it is important for the robotic exoskeleton to be controlled in accordance with the human bio-signal feedback. In order to activate the robot according to the user's motion intention in real time, the robot must to understand the motion intention of the user [8]. In [9], the inverse model of the exoskeleton robot can be used to derive the joint torques. For rehabilitation, designated motion is basically generated with motion controller for the user before their motion.

The developed upper-limb robot-assisted rehabilitation is with high precision for co-manipulation tasks between human and robot. However, the development of an accurate dynamic model of the robot is extremely challenging because of the compliance and oscillations inherent in harmonic drive systems. Modeling of robot dynamics for the purpose of trajectory tracking using low-feedback gains has been studied previously for industrial manipulators. The novelty of this work is the development of rehabilitation robot and adaptive neural network modeling the parameters of a harmonic drive transmission in the robot to facilitate motion control. We have conducted the experiments on human body to identify the various parameters of the harmonic drive system combining sEMG information signals.

Fig. 1. Final version of exoskeleton

2 The Development of Upper Limb Exoskeleton

The developed robot follows the kinematic structure of the human upper limb and spans the elbow and wrist joints (see Fig. 1). It exhibits three degrees- of-freedom corresponding to elbow flexion-extension, forearm pronation-supination, and wrist flexion-extension, which is based upon the behavior of those physiological joints as hinges. Articulation of the developed exoskeleton is achieved about five single-axis revolute joints. The exoskeletal joints are labeled 1 through 5 from proximal to distal in the order.

3 Boosting-Based EMG Patterns Classification

MCLPBoost is inherently of multi-class for the random decision tree. Combining classifiers is a classic trick in pattern recognition field to make robust classifiers. Data comes in records of form $(X, Y) = (x_1, \cdots, x_n, Y)$, where the dependent variable, Y, is the target variable that we are trying to classify and the vector X is composed of the input variables, x_1, x_2, x_3 etc... A tree can be "learned" by splitting the source set into subsets based on an attribute value test. The details of train and prediction process are illustrated in Figs. 2 and 3, respectively. Before training, we first get the feature vector of a sample, which is labeled manually.

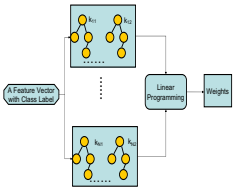

Fig. 2. The train process of MCLPBoost

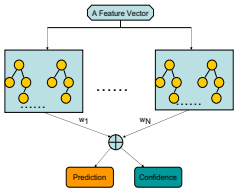

Fig. 3. The prediction process of MCLPBoost

Then, each tree is updated by each sample k times, where k is generated by Poisson distribution. Each tree is initialized as only one root node. A node contains the label density of each class, denoted by $p = \{p_1, \cdots, p_K\}$, where K is the number of classes. As a result, the density set p will be separated into two groups: $p^l = \{p_1^l, \cdots, p_K^l\}$ and $p^r = \{p_1^r, \cdots, p_K^r\}$. In order to select the best test, a measurement is given as $Score = m_l \times \sum_{i=1}^{K} p_i^l(1-p_i^l) + m_r \times \sum_{i=1}^{K} p_i^r(1-p_i^r)$, where $Score$ represents the importance of the test inversely; m_l and m_r denote the number of samples falling left and right respectively.

The linear programming problem in Fig. 2 is different from the original LPBoost algorithm for its ability of training online $\min_{w_t,\xi} C \sum_{k \neq y} \xi_k + \|w_t\|_1$, $s.t.\ \forall n :$ $w_{t,n} \geq 0$, $\forall k \neq y :\ \xi_k \geq 0$, $\forall k \neq y :\ (G_t(y,\cdot) - G_t(k,\cdot))w_t + \xi_k \geq 1$, where C is a designed parameter to limit the overfitting problem. In order to solve the optimization problem, its augmented Lagrangian dual formulation can be described in Eq. (3).

$$\max_{w_t, d_{y'}^n} d_{y'}^n + \sum_{n=1}^{N} w_{t,n}(1 - d_{y'}^n \Delta G_{y'}(n) - \zeta_n) - \frac{1}{2\theta} \sum_{n=1}^{N} (1 - d_{y'}^n \Delta G_{y'}(n) - \zeta_n)^2 \quad (1)$$

$$s.t.\ \forall n :\ \zeta_n \geq 0, w_{t,n} \geq 0 \quad (2)$$

$$0 \leq d_{y'} n \leq C \quad (3)$$

where $\Delta G_{y'}(n) = G(y,n) - G(y',n)$, $d_{y'}^n$ is the sample weight corresponding to the n-th weak learner which outputs the smallest margin on the non-target

class y', ζ is a new set of slack variables, and $\theta > 0$ is a designed constant. In an iterative way, when a new sample arrives, for the first weak learner, we just assign a constant as its sample weight, but for training the n-th ($n > 1$) weak learner, we compute $d_{y'}^n$ by

$$q_j = 1 - d_{y'}^n \Delta G_{y'}(j) - \theta w_{t,j} \tag{4}$$

$$f = d_{y'}^n + \nu_d (1 + \frac{1}{\theta} \sum_{j=1, q_j<0}^{n-1} q_j \Delta G_{y'}(j)) \tag{5}$$

$$d_{y'}^n = \max(0, \min(C, f)) \tag{6}$$

where q_j and f are temporary variables for calculating $d_{y'}^n$, and ν_d is the dual learning rate. Once the sample weight is obtained, we can calculate each weight of the weak learners.

$$\forall n: \; z_n = w_{t,n} - \nu_p (1 - d_{y'}^n \Delta G_{y'}(j)) \tag{7}$$

$$w_{t,n} = \max(0, z_n) \tag{8}$$

where z_n is a temporary variable to calculate $w_{t,n}$, ν_p is the learning rate for the primal. In Eq. (8), it's obvious that the weight of the weak learner, whose margin $\Delta G_{y'}(j))$ is lager, will get a bigger weight.

In contrast to the classifier training process, the prediction (Fig. 3) is relatively simpler. It can be summarized in the following equations.

$$p_n(k|x) = \frac{1}{T} \sum_{t=1}^{T} p_t(k|x) p(k|x) = \frac{1}{N} \sum_{n=1}^{N} w_i p_n(k|x) O(x) = arg \max_k p(k|x) \tag{9}$$

where T denotes the number of trees in a forest; p_t and p_n denote the confidence of the output of a tree and a forest (i.e., one weak learner), respectively, p is the confidence of final output, and O is the prediction.

4 Control Development

The MIMO nonlinear system dynamics can be described as

$$Y^{(r)} = F(x) + G(x)U \tag{10}$$

where $F(x)$ and $G(x)$ is unknown nonlinear function, U and Y is input and output vectors. Assume that $G(x)$ is a positive definite matrix, the desired position is $y_{di}(t)$ and its derivative of η_i order exists, thus define

$$e_i(t) = y_{di}(t) - y_i(t); \tag{11}$$

$$S_i(t) = (\frac{d}{d_t} + \lambda_i)^{\eta_i - 1} e_i(t), \lambda_i > 0; \tag{12}$$

and if $S_i(t) \to 0$, then we also have $e_i(t) \to 0$. According to Newton's binomial theorem, we can decompose $\dot{S}_i$ and get

$$\dot{S} = \zeta - F(x) - G(x)u; \tag{13}$$

$$u = G^{-1}(x)(-F(x) + \zeta + K_0 S); \tag{14}$$

where $\zeta = y_{d_i}^{r_i} + \sum_{j=1}^{r_i-1} \frac{(r_i-1)!}{(r_i-j)!(j-1)!} e_i^{(j)}(t)\lambda_i^{r_i-j}$ and $K_0 = diag[k_{01}, k_{02}, \ldots, k_{0p}]$, $k_{0i} > 0$. Substitute Eq.(13) with Eq.(14) we get $\dot{S}(t) = -K_0 S(t)$. The solution of the differential equation is $s_i(t) = s_i(0)e^{-k_{0i}t}$, with $t \to \infty, s_i(t) \to 0$. If we known the nonlinear function $F(x)$ and $G(x)$, we can get the control output u easily; If not, we can design a fuzzy function to approach the two functions as $y(x) = \xi^T(x)\Theta$; where $\Theta = [\theta^1, \ldots, \theta^M]^T$ is parameters vector, $\xi(x) = [\xi_1(x), \ldots, \xi_M(x)]$, and

$$\xi_l(x) = \frac{\prod_{i=1}^{n} \mu_{F_i^l}(x_i)}{\sum_{l=1}^{M}(\prod_{i=1}^{n} \mu_{F_i^l}(x_i))} \tag{15}$$

The output of the system $y(x)$ converges gradually to the unknown nonlinear function $f_i(x)$ and $g_{ij}(x)$. θ_{f_i} and $\theta_{g_{ij}}$ are the corresponding adaptive regulator parameters. Define the optimal approximation parameters as $\theta_{f_i}^*$ and $\theta_{g_{ij}}^*$. Then we design the $\hat{F}(x, \theta_f)$ and $\hat{G}(x, \theta_g)$ to substitute the $F(x)$ and $G(x)$.

The adaptive control law Θ of the corresponding fuzzy system can be defined as follows

$$\dot{\Theta}_{f_i} = -\eta_{f_i}\xi_{f_i}(x)s_i; \tag{16}$$

$$\dot{\theta}_{g_{ij}} = -\eta_{g_{ij}}\xi_{g_{ij}}(x)s_i u_{cj}; \tag{17}$$

where $\eta_{f_i} > 0, \eta_{g_{ij}} > 0$. Then we substitute $\hat{F}(x, \theta_f)$ and $\hat{G}(x, \theta_g)$ into Eq.(14); we have the control equation as

$$u_c = \hat{G}^{-1}(x)(-\hat{F}(x) + \zeta + K_0 S); \tag{18}$$

To ensure the $\hat{G}(x, \theta_g)$ is nonsingular, we substitute it with a generalized inverse $\chi = \hat{G}^T(x, \theta_g)[\tau_0 I_p + \hat{G}(x, \theta_g)\hat{G}^T(x, \theta_g)]^{-1}$; where τ_0 is a small positive real number randomly, I_p is a unit matrix; Thus, the control input can be expressed as Eq.(19) and the control development is done.

$$u_c = \chi(-\hat{F}(x) + \zeta + K_0 S); \tag{19}$$

To reduce the modeling errors, we take robust control u_r. Thus $u = u_c + u_r$. Where $u_r = \frac{s|s^T|(\bar{\varepsilon}_f + \bar{\varepsilon}_g|u_c| + |u_0|)}{\sigma_0\|s\|^2 + \delta}$; $u_0 = \varepsilon_0[\varepsilon_0 I_p + \hat{G}(x, \theta_g)\hat{G}^T(x, \theta_g)]^{-1}(-\hat{F}(x, \theta_f) + \zeta + K_0 s)$; and the δ is a time-variable parameter.

$$\dot{\delta} = -\eta_0 \frac{|s^T|(\bar{\varepsilon}_f + \bar{\varepsilon}_g|u_c| + |u_0|)}{\sigma_0\|s\|^2 + \delta}; \tag{20}$$

where $\eta_0 > 0, \delta(0) > 0$.

5 Experiments

In this section, the human limb itself, can be used as control interface for the exoskeletons. EMG signals correspond to muscle activity when the muscle contracts. We can obtain sEMG signal from the sEMG sensor system which is fixed with signal amplifier. The amplifier could receive 8 channel of sEMG signal at the same time. The recorded sEMG signal of the wrist and elbow joint has been pre-processde (e.g. amplification, filtering) and post-processed (e.g. smoothing).

5.1 Data Processing

The process of data processing in our experiment can be divided into three phases: feature extraction, feature reduction and classification. In our experiment, the data collected stored in the file folder of Record are used as training data and the data collected online are used as test data. And the classification result consists of three states which was labeled as $0, 1, 2$ in the experiment. And it's can be concluded that all emg signals recorded in the procedure have been classified correctly (see Fig. 4 and 5). Then we use the generated classification to determine the motion of the corresponding motor. In the paper, the desired trajectory is set $q_d = A * (1 - \cos t)$ when the muscle of corresponding joint flexion flex and $q_d = -A * (1 - \cos t)$ when it extent, where q_d is the desired trajectory, A is the positive amplitude of the trajectory. The experiment results using the neural network control are shown in Figs. 6–9. The trajectories of the weights Θ are listed in Figs.11–13. For comparison, the experiments using PD control are shown in Figs. 14–17. From these comparison, we can see the neural network is with good performance.

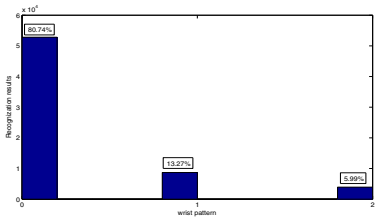

Fig. 4. The result of classification of wrist

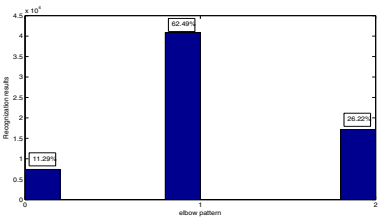

Fig. 5. The result of classification of elbow

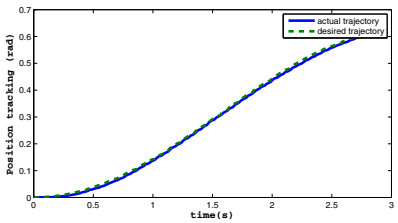

Fig. 6. The tracking of upward wrist

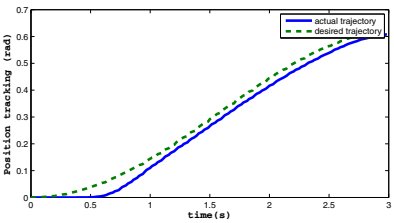

Fig. 7. The tracking of upward elbow

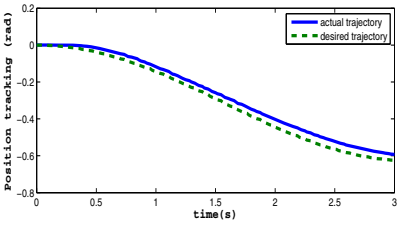

Fig. 8. The tracking of downward wrist

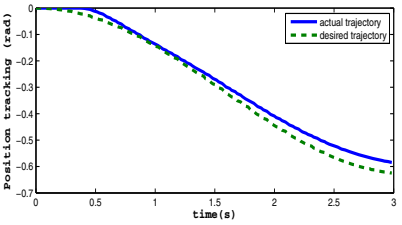

Fig. 9. The tracking of downward elbow

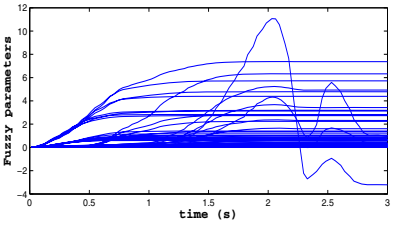

Fig. 10. The weights Θ of upward wrist

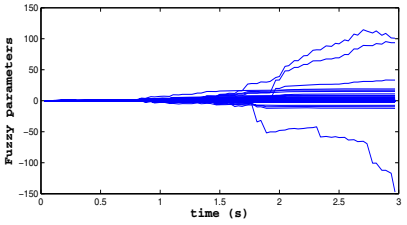

Fig. 11. The weights Θ of upward elbow

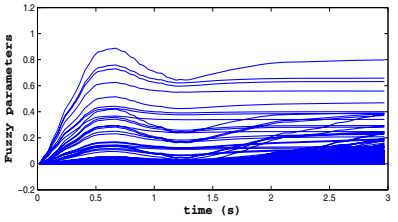

Fig. 12. The weights Θ of downward wrist

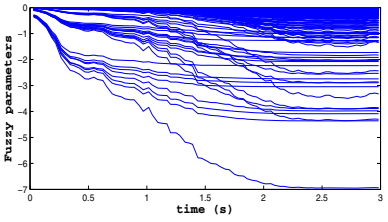

Fig. 13. The weights Θ of downward elbow

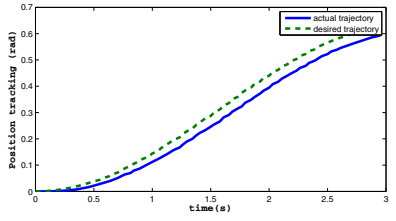

Fig. 14. The PD tracking of upward wrist

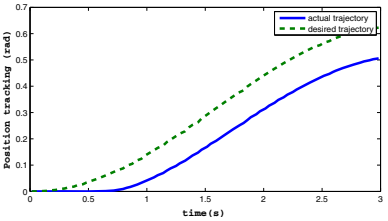

Fig. 15. The PD tracking of upward elbow

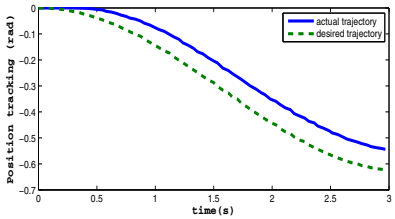

Fig. 16. The PD tracking of downward wrist

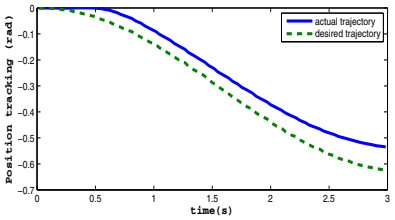

Fig. 17. The PD tracking of downward elbow

6 Conclusions

In this paper, the electromyogram (EMG)-based neural network control of an upper-limb power-assist exoskeleton robot has been developed. The development of an adaptive neural network modeling and control approach to handle the unknown parameters of the harmonic drive transmission in the robot to facilitate motion control. We have conducted the experiments on human subject to identify the various parameters of the harmonic drive system combining sEMG information signals.

References

1. Hallett, M.: Recent advances in stroke rehabilitation. Neurorehabil. Neural Repair 16, 211–217 (2002)
2. Lang, C., Schieber, M.: Differential impairment of individuated finger movements in humans after damage to the motor cortex or the corticospinal tract. J. Neurophysiol. 90, 1160–1170 (2003)
3. Masia, L., Krebs, H., Cappa, P., Hogan, N.: Design, characterization, and impedance limits of a hand robot. In: Proc. IEEE Int. Conf. Robotic Rehabil. (ICORR), pp. 1085–1089 (June 2007)
4. Kahn, L.E., Rymer, W.Z., Reinkensmeyer, D.J.: Adaptive assistance for guided force training in chronic stroke. In: Proceedings of the 26th Annual International Conference of the IEEE Engineering in Medicine and Biology Society, San Francisco, CA, USA, pp. 2722–2725 (2004)
5. Krebs, H.I., Hogan, N., Aisen, M.L., Volpe, B.T.: Robot-aided neurorahabilitation. IEEE Transactions on Rehabilitation Engineering 6(1), 75–87 (1998)
6. Lum, P.S., Burga, C.G., Loos, M.V., Sho, P.C., Majmundar, M., Yap, R.: MIME robotic device for upper-limb neurorehabilitation in subacute stroke subjects: A follow-up study. J. Rehabil. Res. Dev. 43(5), 631–642 (2006)
7. Masiero, S., Celia, A., Rosati, G., Armani, M.: Robotic-assisted rehabilitation of the upper limb after acute stroke. Arch. Phys. Med. Rehabil. 88(2), 142–149 (2007)
8. Kong, K., Jeon, D.: Design and control of an exoskeleton for the elderly and patients. IEEE/ASME Trans. Mechatronics 11(4), 428–432 (2006)
9. Kazerooni, H., Steger, R.: The Berkeley lower extremity exoskeleton. Trans. ASME, J. Dyn. Syst., Meas. Control 128(1), 14–25 (2006)